

Organization of Motor Proteins into Functional Micropatterns Fabricated by a Photoinduced Fenton Reaction**

Maniraj Bhagawati, Surajit Ghosh, Annett Reichel, Klaus Froehner, Thomas Surrey, and Jacob Piehler*

The functional organization of proteins on solid supports is a key prerequisite for the integration of the powerful capabilities of biomolecules into miniaturized biomedical and biotechnological devices.^[1] Motor proteins are particularly attractive building blocks for the construction of such devices. Numerous approaches have been reported for the organization of motor proteins into functional micro- and nanostructures,^[2–8] which have inspired the development of novel bioanalytical devices.^[9–13] For these purposes, techniques for the functional organization of proteins on surfaces into micrometer- and submicrometer-sized assemblies are required.

Despite substantial developments in this field, simple and generic techniques for functional protein patterning are scarce.^[14] A critical prerequisite is that the functionality of proteins immobilized on the surface must be fully maintained. As many proteins denature upon interaction with solid supports, surface modifications, for example, in the form of thin protein-repellent polymer layers, are required to render the surface biocompatible. Moreover, suitable, spatially resolved functionalization of these layers is required for the site-specific capturing of target molecules onto the surface.^[14] We previously developed multivalent head groups containing nitrilotriacetic acid (NTA) moieties (such as tris-NTA, Figure 1 a) as generic, high-affinity adapters for oligohistidine-tagged proteins.^[15] These multivalent chelators have proven powerful for stable, yet reversible protein binding in solution and for immobilization onto various supports.^[16–18] Through the use of such chelators in combination with a dense poly(ethylene glycol) (PEG) polymer brush, we demonstrated the oriented capturing of highly active kinesin on glass surfaces.^[19] Herein, we present a generic method for the

functional micropatterning of such surface architectures. This method is based on selective photodestruction by a light-induced Fenton reaction (Figure 1 b), whereby suitable transition-metal ions are complexed by the immobilized NTA moieties.

For the implementation of this approach, we used both UV illumination through a mask and the UV laser of a standard confocal microscope. The principle of the first technique is depicted schematically in Figure 1 c: After loading of the NTA moieties with Co^{II} ions, the surface is illuminated with UV light through a mask. All metal ions are then removed by washing with HCl or ethylenediaminetetraacetic acid (EDTA), and the remaining NTA groups are loaded with Ni^{II} ions prior to protein binding.

The protein-binding efficiencies of tris-NTA-functionalized surfaces after UV illumination with the NTA moieties loaded with different transition-metal ions are compared in Figure 1 b. Illumination in the presence of Ni^{II} ions did not affect the binding capacity of the surface; in contrast, no protein binding was observed after illumination of surfaces loaded with Co^{II} , Cu^{I} , or Fe^{II} ions. These three transition-metal ions mediate photoinduced Fenton reactions,^[20–22] which are probably responsible for the destruction of the NTA moieties on the surface. The same effect was observed for surfaces functionalized with mono-NTA. A decrease in the efficiency of photodestruction on surfaces was observed when the length of the PEG chain was decreased (see the Supporting Information). Thus, the surface architecture has some influence on the destruction process.

To further characterize the photodestruction process, we quantitatively assessed protein binding to surfaces after illumination for shorter periods of time than required for full destruction of the binding capacity. The unstable protein binding observed under these conditions (see the Supporting Information) indicated that the tris-NTA groups were partially destroyed and thus lost binding affinity. Moreover, leaching of Ni^{II} ions was observed, which indicated that the NTA moieties themselves were decomposed by the Fenton reaction. This result is in line with studies carried out on the hydroxyl-radical-mediated oxidation of chelating agents such as NTA and EDTA. The oxidation of NTA yielded species with a weaker metal-ion-coordination ability, such as imidodiacetic acid, glycolic acid, oxalic acid, and glycine.^[23] Since the active oxidant in the Fenton reaction is also a hydroxyl radical, a similar oxidation pathway can be assumed. Thus, the metal-ion-mediated photodestruction appears to selectively eliminate the transition-metal-ion-binding moieties, but not the protein-repelling PEG polymer brush. This conclusion is

[*] M. Bhagawati,^[†] A. Reichel, Prof. Dr. J. Piehler
Institut für Biophysik, Universität Osnabrück
Barbarastrasse 11, 49076 Osnabrück (Germany)
Fax: (+49) 541-9692262
E-mail: piehler@uos.de
Homepage: <http://www.biologie.uni-osnabrueck.de/Biophysik/Piehler/>

Dr. S. Ghosh,^[†] Dr. T. Surrey
Cell Biology and Biophysics Unit, EMBL Heidelberg (Germany)
K. Froehner
NB Technologies, Bremen (Germany)

[†] These authors contributed equally.

[**] We thank Mathias Utz and Gerhard Spatz-Kümbel for technical assistance, and Christian Henrich and Dr. Peter Bieling for advice and reagents. This project was supported by the BMBF (0312034).



Supporting information for this article is available on the WWW under <http://dx.doi.org/10.1002/anie.200904576>.

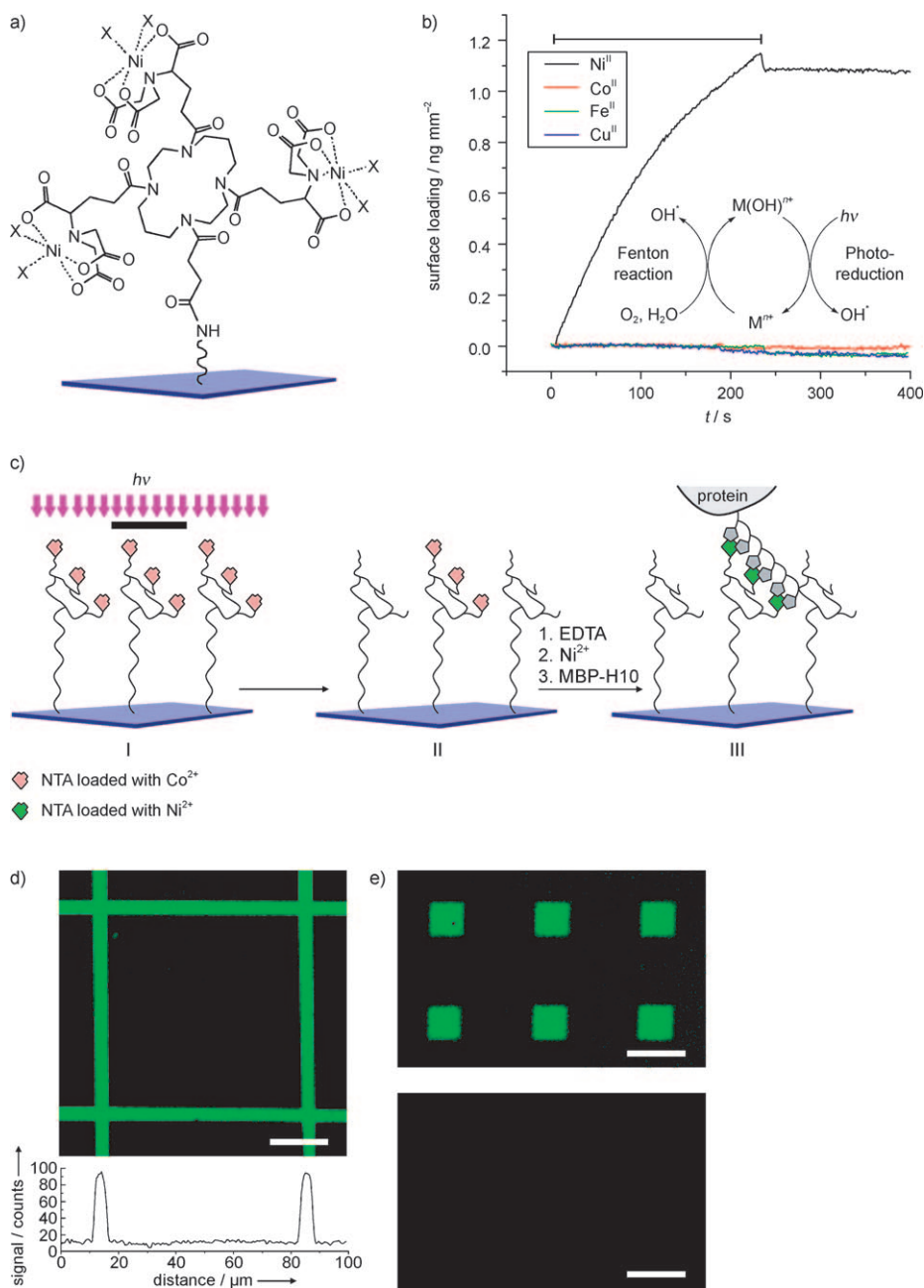


Figure 1. Photodestruction of NTA-functionalized surfaces by a light-induced Fenton reaction. a) Structure of Ni^{II}-loaded tris-NTA attached to a PEG polymer brush. The free coordination sites for capturing oligohistidine moieties are indicated by “X”. b) Binding of the His-tagged protein MBP-H10 to tris-NTA surfaces after UV illumination in the presence of different transition-metal ions and subsequent loading of the remaining NTA groups with Ni^{II} ions. Protein binding was detected by reflectance interference. The mechanism of the light-induced Fenton reaction is also shown. c) Schematic illustration of the patterning process: I) UV irradiation through a photomask of surfaces modified with tris-NTA head groups, which have been loaded with Co^{II} ions; II) tris-NTA head groups exposed to UV irradiation are destroyed; III) remaining tris-NTA head groups can capture His-tagged proteins after loading with Ni^{II} ions. d) Functional surface micropatterning by illumination through a mask. The remaining tris-NTA moieties were loaded with fluorescence-labeled MBP-H10 and imaged by confocal laser scanning microscopy. e) Binding of fluorescence-labeled IFNα₂ to micropatterned surfaces with (top) and without (bottom) prior incubation of its His-tagged receptor IFNAR2. The scale bar is 20 μm in all images.

supported by the observation of negligible nonspecific protein binding to surfaces after photodestruction (Figure 1b).

sities of binding sites (Figure 2c) and thus provided the possibility to control the surface concentration of immobi-

This approach turned out to be promising for functional surface micropatterning: after UV illumination through a mask, the selective and fully reversible binding of fluorescence-labeled, decahistidine-tagged maltose binding protein (MBP-H10) to the areas that had not been illuminated was observed by confocal laser scanning microscopy (Figure 1d). We explored the specificity of protein binding as well as the functionality of the immobilized protein with a protein–protein interaction assay (Figure 1e). For this purpose, the protein interferon α₂ labeled with Oregon Green 488 (^{OG488}IFNα₂, without a His tag) was incubated on a micropatterned surface with and without prior incubation of its receptor IFNAR2 fused to a decahistidine tag (IFNAR2-H10). The binding of ^{OG488}IFNα₂ into micropatterns was observed only in the presence of IFNAR2-H10. This experiment thus confirmed the highly specific protein binding as well as the functional integrity of proteins immobilized into such micropatterns.

In the second approach, we explored the in situ patterning of tris-NTA-functionalized surfaces with the 405 nm laser beam of a confocal laser scanning microscope (Figure 2a). We carried out the photodestruction of Co^{II}-loaded tris-NTA by scanning selected regions of interest with the beam of the 405 nm laser either in the presence of ^{OG488}MBP-H10 for focusing purposes (Figure 2a) or without the protein. After the removal of Co^{II}, the surfaces were loaded with Ni^{II} ions, and the binding of ^{OG488}MBP-H10 was imaged. Selective photodestruction occurred in the illuminated areas (Figure 2b). Photodestruction by a light-induced Fenton reaction was confirmed by several control experiments (see the Supporting Information). Variation of the number of iteration cycles during exposure to the 405 nm laser yielded different den-

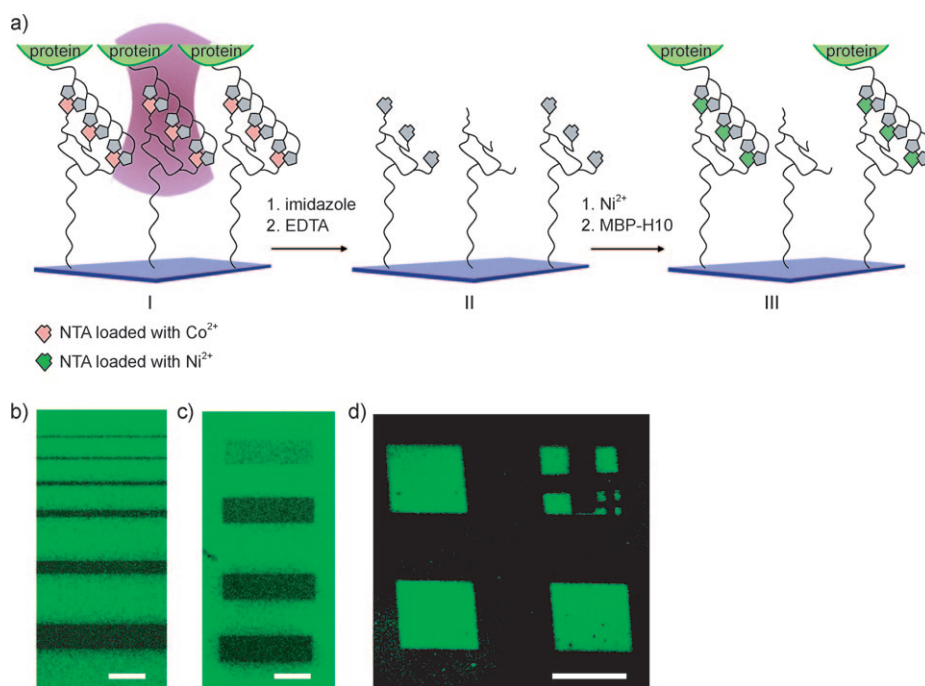


Figure 2. In situ patterning of tris-NTA surfaces. a) Schematic illustration of the process: I) photo-destruction of Co^{II} -loaded tris-NTA (to which a protein may be bound); II) removal of Co^{II} ions (and the protein, if applicable) with imidazole and EDTA; III) loading of proteins onto intact areas after loading with Ni^{II} ions. b) Lines of different width were scanned with the 405 nm laser in the presence of NTA-complexed Co^{II} ions. c) Protein binding to surfaces with rectangular structures scanned in the presence of NTA-complexed Co^{II} ions with the 405 nm laser for different numbers of iterations (from top: 10, 50, 100, 200). d) Pattern obtained by illumination through a mask and further modification of the square in the upper right corner by confocal laser scanning. Scale bar is 20 μm in all images.

lized proteins in a spatially resolved manner. The two approaches for surface patterning can be combined readily, as depicted in Figure 2d: Patterns created by illumination through a mask were subsequently modified further by confocal scanning with a 405 nm laser beam as described above.

Next, we used our photochemical surface-patterning method to immobilize molecular motors into microstructures and tested whether they supported guided filament transport. For this purpose, we used a recombinant dimeric kinesin with a C-terminal decahistidine tag (kinesin-H10) that had been shown before to support microtubule gliding on unpatterned tris-NTA surfaces.^[19] We coimmobilized decahistidine-tagged green fluorescent protein (GFP-H10) as a fluorescent marker to visualize the tris-NTA lines. Alexa568-labeled microtubules landed selectively on the kinesin/GFP lines in random orientations (Figure 3a,b). In the presence of adenosine triphosphate (ATP), all microtubules in contact with the lines were transported by the motors, thus confirming that photochemical patterning followed by subsequent selective tris-NTA-mediated motor immobilization yields highly active protein patterns. Microtubules which had landed perpendicularly to the line diffused into solution after having been transported out of the line region.

Microtubules with a parallel orientation with respect to the line were observed to glide along the line (Figure 3c; see

movie 1 in the Supporting Information); in most cases they glided distances several times their length (Figure 3c). Quantitative analysis revealed that the distance traveled on individual lines was influenced by the characteristics of the pattern. Microtubules were observed to systematically travel slightly longer distances on thinner lines (Figure 3d). The very small difference in the velocities of the microtubules gliding on the two types of lines studied ($360 \pm 60 \text{ nm s}^{-1}$ on 1 μm wide lines and $370 \pm 60 \text{ nm s}^{-1}$ on 5 μm wide lines) confirmed that the motor proteins on both lines had similar densities.^[19] These observations suggest that further reduction of the thickness of these structures to submicron dimensions could lead to even higher microtubule-transport fidelity.

In summary, we have developed a versatile method for functional protein patterning. In contrast to conventional methods, such as the microcontact printing of proteins, our new method is optimized for highly active protein patterns, because the microstructuring reaction takes place at the

level of chemistry, and the biomolecules are captured under physiological conditions. This approach introduces the flexibility to separate patterning and protein immobilization and thus reduce the danger of protein inactivation during patterning. We have used this method to organize motor proteins into highly functional microstructures. Motility assays established that microtubule-transport characteristics depend on geometrical features of the tracks that are defined by the patterning process. The possibility to modify mask-based protein structures by using the additional flexibility of confocal laser scanning provides a means for generating complex patterns, which will enable further exploration of the foundations of microtubule transport by micropatterned motor proteins. However, the generic application of this technique for the functional micropatterning of proteins, including recombinant antibodies or protein ligands for localized cell-surface-receptor activation, is ensured by the widespread use of the His tag for affinity purification.

Received: August 17, 2009

Published online: ■■■■, 2009

Keywords: immobilization · microarrays · molecular devices · protein micropattern · protein–protein interaction

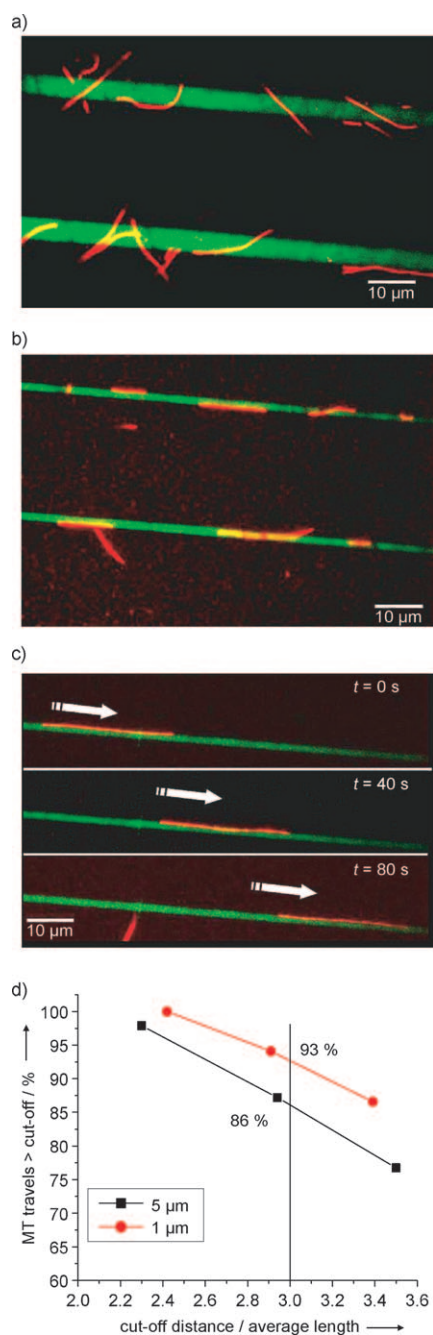







Figure 3. Transport of microtubules by kinesin-H10 immobilized selectively on tris-NTA line patterns. a,b) Fluorescence images of Alexa568-labeled microtubules (red) on kinesin-H10 captured on tris-NTA lines (green) with widths of 5 μm (a) and 1 μm (b). c) Images from a time-lapse movie showing a labeled microtubule (red) on a kinesin-H10–tris-NTA line with a width of 1 μm (green) at the times indicated. d) Percentage of microtubules (MTs) that traveled further than the indicated number of times their average length along lines with widths of 5 μm (red) and 1 μm (black). More than 85% and more than 90% of the microtubules traveled more than three times (vertical line) their average length along lines with widths of 5 μm and 1 μm , respectively.

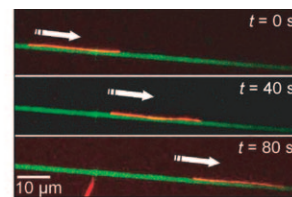
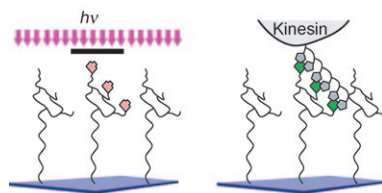
[1] M. G. van den Heuvel, C. Dekker, *Science* **2007**, *317*, 333.
 [2] J. Clemmens, H. Hess, R. Doot, C. M. Matzke, G. D. Bachand, V. Vogel, *Lab Chip* **2004**, *4*, 83.
 [3] H. Hess, C. M. Matzke, R. K. Doot, J. Clemmens, G. D. Bachand, B. C. Bunker, V. Vogel, *Nano Lett.* **2003**, *3*, 1651.
 [4] J. Clemmens, H. Hess, C. Matzke, G. Bachand, B. Bunker, V. Vogel, *Biophys. J.* **2003**, *84*, 293A.
 [5] H. Hess, J. Clemmens, D. Qin, J. Howard, V. Vogel, *Nano Lett.* **2001**, *1*, 235.
 [6] C. Reuther, L. Hajdo, R. Tucker, A. A. Kasprzak, S. Diez, *Nano Lett.* **2006**, *6*, 2177.
 [7] L. Ionov, M. Stamm, S. Diez, *Nano Lett.* **2006**, *6*, 1982.
 [8] Y. M. Huang, M. Uppalapati, W. O. Hancock, T. N. Jackson, *Biomed. Microdevices* **2007**, *9*, 175.
 [9] T. Kim, L. J. Cheng, M. T. Kao, E. F. Hasselbrink, L. Guo, E. Meyhofer, *Lab Chip* **2009**, *9*, 1282.
 [10] L. Rios, G. D. Bachand, *Lab Chip* **2009**, *9*, 1005.
 [11] T. Fischer, A. Agarwal, H. Hess, *Nat. Nanotechnol.* **2009**, *4*, 162.
 [12] A. Goel, V. Vogel, *Nat. Nanotechnol.* **2008**, *3*, 465.
 [13] C. T. Lin, M. T. Kao, K. Kurabayashi, E. Meyhofer, *Nano Lett.* **2008**, *8*, 1041.
 [14] C. You, M. Bhagawati, A. Brecht, J. Piehler, *Anal. Bioanal. Chem.* **2009**, *393*, 1563.
 [15] S. Lata, A. Reichel, R. Brock, R. Tampé, J. Piehler, *J. Am. Chem. Soc.* **2005**, *127*, 10205.
 [16] S. Lata, M. Gavutis, J. Piehler, *J. Am. Chem. Soc.* **2006**, *128*, 6.
 [17] A. Tinazli, J. Tang, R. Valiokas, S. Picuric, S. Lata, J. Piehler, B. Liedberg, R. Tampe, *Chemistry* **2005**, *11*, 5249.
 [18] S. Lata, J. Piehler, *Anal. Chem.* **2005**, *77*, 1096.
 [19] P. Bieling, I. A. Telley, J. Piehler, T. Surrey, *EMBO Rep.* **2008**, *9*, 1121.
 [20] P. Ciesla, P. Kocot, P. Mytych, Z. Stasicka, *J. Mol. Catal. A* **2004**, *224*, 17.
 [21] N. K. Urbanski, A. Beresewicz, *Acta Biochim. Pol.* **2000**, *47*, 951.
 [22] S. Leonard, P. M. Gannett, Y. Rojanasakul, D. Schwegler-Berry, V. Castranova, V. Vallyathan, X. Shi, *J. Inorg. Biochem.* **1998**, *70*, 239.
 [23] C. Emilio, R. Gettar, M. Litter, *J. Appl. Electrochem.* **2005**, *35*, 733.

Communications

Surface Patterning

M. Bhagawati, S. Ghosh, A. Reichel,
K. Froehner, T. Surrey,
J. Pehler*     

Organization of Motor Proteins into
Functional Micropatterns Fabricated by a
Photoinduced Fenton Reaction



Walking the line: Selective photodestruction of nitilotriacetic acid moieties on a poly(ethylene glycol) polymer brush by a light-induced Fenton reaction enabled the functional organization of motor proteins

into micropatterns (see schematic illustration). Microtubules were selectively captured on the structures, and adenosine triphosphate dependent transport along lines was observed.